Energy Conversion and Management 92 (2015) 287–301

Contents lists available at ScienceDirect

Energy Conversion and Management

journal homepage: www.elsevier.com/locate/enconman

Smart microgrid hierarchical frequency control ancillary service provision based on virtual inertia concept: An integrated demand response and droop controlled distributed generation framework

Navid Rezaei, Mohsen Kalantar *

Center of Excellence for Power Systems Automation and Operation, Electrical Engineering Department, Iran University of Science and Technology (IUST), Narmak, Tehran 16846 13114, Iran

ARTICLE INFO

Article history:
Received 3 October 2014
Accepted 15 December 2014
Available online 9 January 2015

Keywords:
Microgrid energy management system
Droop control
Virtual inertia
Reserve scheduling
Demand response

ABSTRACT

Low inertia stack, high penetration levels of renewable energy source and great ratio of power deviations in a small power delivery system put microgrid frequency at risk of instability. On the basis of the close coupling between the microgrid frequency and system security requirements, procurement of adequate ancillary services from cost-effective and environmental friendly resources is a great challenge requests an efficient energy management system. Motivated by this need, this paper presents a novel energy management system that is aimed to coordinately manage the demand response and distributed generation resources. The proposed approach is carried out by constructing a hierarchical frequency control structure in which the frequency dependent control functions of the microgrid components are modeled comprehensively. On the basis of the derived modeling, both the static and dynamic frequency securities of an islanded microgrid are provided in primary and secondary control levels. Besides, to cope with the low inertia stack of islanded microgrids, novel virtual inertia concept is devised based on the precise modeling of droop controlled distributed generation resources. The proposed approach is applied to typical test microgrid. Energy and hierarchical reserve resource are scheduled precisely using a scenario-based stochastic programming methodology. Moreover, analyzing the results verifies the impressiveness of the proposed energy management system in cost-effectively optimizing the microgrid ancillary service procurement.

1. Introduction

Economic-environmental motivations to provide the ever-increasing energy demands in a secure and reliable framework lead the power system operators to utilize Distribute Energy Resources (DERs) more than ever [1]. On the other hand, individual uncoordinated operation of the DERs particularly Renewable Energy Sources (RESs) may have deteriorative impacts on the power system stability, sustainability and power quality indices [2]. In this regard, microgrid idea as an active and controllable infrastructure have been introduced as a reliable ground to aggregate various DER technologies and loads together in a small distribution power system [3]. Microgrids have also a high potential to facilitate the active participation of the end-user consumers in the light of the Demand Response (DR) programs [4]. Microgrid central controller (MGCC) can exploit the DR programs in order to not only reduce energy costs but also to provide the high level reliability and security requirements [5].

Microgrids are met with new complicated challenges stem from more complex components and higher degrees of uncertainty in a small region of power system. The challenges are more critical in the islanded mode and directly threaten the microgrid frequency security. In other words, unlike the synchronous generators, most of the DER units require static Voltage Source Inverter (VSI) units to connect to the grid in a sustainable manner. As a result, arisen from the lower inertia of the VSIs, not only the loadability and stability capabilities of the microgrid are reduced [6] but also the control system complexity is strengthened [7]. Besides, the intermittency of the RES units produces an uncertain operational environment for the islanded microgrids. The power fluctuations arise from the unpredictable load consumption also augments the degree of the uncertainty [8]. Thus, the control and management of the microgrid frequency security, particularly in the islanded mode, is a great challenge which should be investigated

* Corresponding author. Tel.: +98 21 73225662; fax: +98 21 73225662.
E-mail addresses: nrezaei@iust.ac.ir (N. Rezaei), kalantar@iust.ac.ir (M. Kalantar).

http://dx.doi.org/10.1016/j.enconman.2014.12.049
0196-8904/

Nomenclature

Acronyms

DER	Distributed Energy Resource
DG	Distributed Generation
DR	Demand Response
DRP	Demand Response Provider
ELNS	Expected Load not supplied
EMS	Energy Management System
MCS	Monte Carlo Simulation
MGCC	Micro-Grid Central Controller
MILP	Mixed Integer Linear Programming
PV	Photovoltaic
RCF	Rate of Change of Frequency
RES	Renewable Energy Source
RWM	Roulette Wheel Mechanism
TEF	Total Expected Frequency
TOC	Total Operation Cost
TOE	Total Operation Emission
VSI	Voltage Source Inverter
VOLL	Value Of Lost Load
WT	Wind Turbine

Indices

i	index of VSI based DG from 1 to Ng
w	index of wind turbines from 1 to Nw
v	index of photovoltaic panels from 1 to Nv
d	index of demand response providers from 1 to Nd
s	index of random scenarios from 1 to Ns
h	index of hours from 1 to Nh
l	index of frequency control level could be pri (primary) and *sec* (secondary)
ud	index of scheduled reserves could be *up* or *down*

Parameters and Constants

$m_{p,i}$	frequency droop control gain of i-th VSI-based DG
f_{ref}	microgrid reference frequency
$\Delta f_l^{\max}$	maximum allowable microgrid frequency excursion limit during control level l
$\text{ROCOF}_{\text{MG}}^{\max}$	maximum allowable microgrid rate of change of frequency limit
$\text{ROCOF}_i^{\max}$	maximum allowable rate of change of frequency limit associated to i-th DG
a_i	fixed operation cost of i-th VSI based DG
b_i	first-order operation cost of i-th VSI based DG
$H_{V,i}$	virtual inertia constant of i-th VSI based DG
$\omega_{c,i}$	low-pass filter cut-off frequency of i-th VSI based DG
$\rho_{i,l,ud}^R$	cost of up/down reserve of i-th VSI based DG in control level l
$\alpha_{d,m}^E$	cost of energy offer of m-th block in d-th DRP price-demand curve
$\alpha_{d,l,ud}^R$	cost of up/down reserve of d-th DRP in control level l
ρ_w	cost of operation of wind turbine w
ρ_v	cost of operation of photovoltaic panel v
E_i^g	CO_2 emission rate of i-th VSI based DG
$P_i^{\max}$	upper level of active power generation of i-th VSI based DG
$P_i^{\min}$	lower level of active power generation of i-th VSI based DG
$P_{L,h}$	forecasted load consumption at hour h
$P_{w,h}$	forecasted active power output of wind turbine w at hour h
$P_{v,h}$	forecasted active power output of photovoltaic panel v at hour h

Variables

π_s	probability of scenario s
$\Delta f_{l,h}^s$	microgrid frequency excursion in scenario s, control level l and at hour h
$\Delta P_{i,l,h}^s$	active power deviation of i-th VSI based DG in scenario s, control level l and hour h
$\Delta P_{w,l,h}^s$	active power deviation of wind turbine w in scenario s, control level l and hour h
$\Delta P_{v,l,h}^s$	active power deviation of photovoltaic panel v in scenario s, control level l and hour h
$\Delta P_{\text{ref},i,l,h}^s$	reference power deviation of i-th VSI based DG in scenario s, control level l and hour h
$P_{i,h}$	active power output of i-th VSI based DG at hour h
$D_{L\text{-}l,h}^s$	frequency elasticity of microgrid loads in scenario s, control level l and hour h
$P_{\text{ref},i,h}$	reference power set point of i-th VSI based DG at hour h
$R_{i,l,ud,h}$	scheduled up/down reserve of i-th VSI based DG in control level l and hour h
$u_{i,h}^l$	binary variable indicating commitment state of i-th VSI based DG at hour h and control level l
$u_{i,h}$	binary variable indicating commitment state of i-th VSI based DG at hour h
$\Delta f_{l,h}^s$	microgrid frequency excursion in scenario s, control level l at hour h
$\text{ROCOF}_{\text{MG},h}^s$	rate of change of frequency of microgrid in scenario s at hour h
$\text{ROCOF}_{i,h}^s$	rate of change of frequency of i-th VSI-based DG in scenario s at hour h
$P_{d,h}^m$	offered load reduction corresponding to m-th block of d-th DRP at hour h
$P_{d,l,h}^{s,m}$	offered load reduction corresponding to scenario s of m-th block of d-th DRP at hour h
$P_{d,h}$	aggregated offered load reduction corresponding to d-th DRP at hour h
$P_{d,l,h}$	aggregated offered load reduction corresponding to d-th DRP at hour h in control level l
$R_{d,l,ud,h}$	scheduled up/down reserve of d-th DRP in control level l and hour h
$P_{i,l,h}^s$	active power output of i-th VSI based DG in scenario s, control level l and hour h
$P_{\text{ref},i,l,h}^s$	reference power of i-th VSI based DG in scenario s, control level l and hour h
$P_{w,l,h}^s$	active power output of wind turbine w in scenario s, control level l and hour h
$P_{v,l,h}^s$	active power output of photovoltaic panel v in scenario s, control level l and hour h
$P_{L,l,h}^s$	microgrid load consumption in control level l and hour h
$P_{L,l,h,f}^s$	microgrid load contribution in according to natural load-frequency dependency in control level l and hour h at static frequency f
$\text{LSH}_{l,h}^s$	load to be shed unwillingly in scenario s, control level l and hour h

in-depth. Frequency is a common control variable which directly reflects the microgrid security [9]. Improper management of the frequency excursions not only queers the microgrid sustainability but also biases its economic and environmental targets. The interdependent coupling between the microgrid frequency and precise energy and reserve scheduling leads the MGCC to devise an

efficient energy management system (EMS) to provide the microgrid security in a cost-effective manner [10].

The EMS can be appropriately performed under a hierarchical control structure. Inspired from the conventional power systems, the microgrid hierarchical EMS consists of primary, secondary and tertiary control levels [11]. In the islanded operation, the highest control level is the secondary level and the associated control functions are accomplished by means of the MGCC [4]. The MGCC optimizes the microgrid production and consumption while concurrently ensures the techno-economic objectives [12]. The functions of the primary control level mainly stand on the droop control method as a promising and compatible control strategy which has a great consistency with the islanded mode [13]. The droop controlled VSI units are in charge to alleviate the frequency excursions by properly adjusting their generation active power outputs [14]. The MGCC is responsible to manage the primary and secondary control reserves enough that frequency is controlled economically.

To provide the microgrid frequency security in a more reliable and economic-environmental friendly manner, the MGCC can benefit from the potential of the DR programs [15]. In other words, owing to the capability of the DR programs in changing their consumption patterns, especially when the system reliability is in question [16], the coordinated operation of the DR programs and the VSI based Distributed Generation (DG) units causes the microgrid frequency security to be managed through a higher providence.

Authors in [6] investigated the optimal power flow of an islanded MG subject to the loadability and the corresponding droop control constraints. However, the hierarchical reserve scheduling was not taken into account and the MG frequency behavior has not been modeled. Several multi-objective optimization approaches based on heuristic methodologies have been investigated in the literature. Authors in [17] presented a particle swarm optimization based operational planning of a renewable microgrid accompanied by back-up MT/FC/battery for leveling the daily energy mismatches. In [18] a smart energy management system for optimizing the microgrid day-ahead operation has been explored. They employed a matrix real-coded genetic algorithm to achieve a practical methodology for load management and control the outputs of the DERs owing to different operational policies. Likewise, in [19] genetic algorithm has been applied to solve a nonlinear based environmental/economic operational optimization of a residential microgrid. Authors in [20], through a multi-objective optimization based on an efficient bacterial foraging algorithm have optimized the operational costs and emissions of a microgrid taken into account the uncertainty of wind turbines. Ref. [21] based on two phase stochastic programming has proposed an adaptive modified firefly algorithm to seek for optimal operation management of microgrids under the different uncertainties. In [22] an improved teaching–learning inspired algorithm has been employed to schedule the microgrid energy requirements with goals of costs and emissions minimization. Despite that the above mentioned methodologies may be effective their solution may be affected by the drawback of the heuristic algorithms in handling with high constrained problems. Also, [23] aimed to provide an optimal operation management of an islanded microgrid with consideration of ensuring uninterruptable power supply services and reducing the global cost of generated power. Analogously in [24], using a mixed integer nonlinear programming approach (MINLP) the energy management problem of an islanded MG has been carried out in order to maximize the utilization of the DERs with a cheap day-ahead operational cost. However, in the above mentioned references, the great impacts of suddenly load fluctuations or randomly RES power output variations on the MG energy scheduling were disregarded. Also, no attention paid to the procurement of the reserve requirements from the end-user consumers.

In admired work, [25], primary and secondary frequency control loops have been modeled, however, corresponding uncertainty resources were not modeled and MG frequency security requirements were not reported. Moreover, no attention paid to the DR capability in enhancing the microgrid security. In [26], through a stochastic-based optimization, day-ahead energy and reserve resources of a micro-grid have been managed. As well in [27], using some Demand Response Providers (DRPs), the end-user consumers have been participated into the microgrid energy and reserve scheduling. Indeed, if the DRPs' bids have been accepted, they were called to participate into operational planning by adjusting their power consumption. Despite the efficiency of the proposed approaches the frequency dependent behavior of the DERs and its impact on the microgrid reserve scheduling has not been developed. In [28], a novel cost effective frequency-dependent energy management system has been proposed. The static performances of the droop controlled DER units have modeled properly. On the basis of the derived formulation, the day-ahead energy and control reserves have been managed such that both the security and economic objectives have been satisfied. In [28], the authors concentrated on only the static performance of the VSI units and no solution was proposed to cope with the low inertia stack in the microgrid. Noteworthy, the low inertia of the VSI-based DG units has deteriorative impacts on the islanded microgrid dynamic security which should be considered by means of the hierarchical EMS structure.

To cope with the high rate of change of frequency (ROCOF) stem from low inertia of the VSI units, this paper proposes a novel frequency dependent energy management system based on virtual inertia concept. By this way, both the static and dynamic behaviors of the microgrid are modeled thoroughly using the proposed droop control and virtual inertia concepts. In other words, precise scheduling and deployment of the reserve resources request the consideration of the microgrid static and dynamic frequency behavior into the energy management system. To best of our knowledge, no work has taken into account the ROCOF index into the microgrid day-ahead energy and reserve management problem. In order to fill this gap out, using two novel frequency dependent technical indices, the steady-state and dynamic frequency control performances of the VSIs based DERs are modeled in-depth. To ensure the economic and environmental targets of microgrid, two indices have been also formulated based daily operational cost and emission. These indices reflect the economic and environmental policies of the MGCC and controlled in promising levels through the associated cost and emission of the security provision are justified.

Based on the derived modeling, the present paper proposes a new objective function which aims to optimize the microgrid day-ahead frequency profile by suitable managing the microgrid expected frequency excursions and also the ROCOF in a cost-effective scheme. Owing to superior significance of the security provision to the economic-based goals, the main objective of the paper is constructed on the basis of the frequency dependent technical indices. The MGCC manages the VSI-based DG units and DR programs in a coordinated manner through which all fourfold techno-economic and environmental indices are ensured simultaneously. Furthermore, to promote the proposed EMS, a scenario-based stochastic programming is used to cope with the microgrid various uncertainties such as load and RES output variations. In summary, the main contributions of the paper can be highlighted as the followings:

- The static and dynamic frequency securities of an islanded microgrid are formulated in detail based on the droop control and virtual inertia concepts. A novel frequency dependent

objective reflecting the microgrid hourly frequency security is proposed using the expected values of the microgrid frequency excursion and ROCOF indices. Using the proposed objective function, the microgrid frequency security is optimized subject to economic and environmental policies specified by means of the MGCC. Furthermore, the microgrid operational cost and emission levels are assured using two pre-defined economic-based indices.

- The DR and VSI-based DG resources are coordinately managed through a hierarchical energy management system. The end-user consumers are considered into the security provision problem by intermediary of a DRP agency. Besides, to overcome the system uncertainties, energy, primary and secondary control reserves are scheduled precisely using a well-organized scenario-based stochastic programming approach. The scenarios are generated using Monte-Carlo Simulation (MCS) and Roulette Wheel Mechanism (RWM) strategies. To trade-off between computational efficiency and solution accuracy an efficient scenario reduction algorithm is employed. To ensure the solution optimality, the proposed security management problem is solved using an efficient mixed-integer linear programming (MILP) methodology.

The remainder of the paper is organized as follows. Section 2 describes the mathematical formulations of the proposed hierarchical frequency dependent modeling of the microgrid components considering the both static and dynamic security requirements. In Section 3, the proposed new objective function and the associated techno-economic operational constraints are presented. In Section 4, the simulations are performed in a typical test microgrid and the numerical results optimized over a 24 hour scheduling time horizon are reported. In Section 5, an in-depth discussion on the derived results is carried out. Section 6 consists of some relevant conclusion remarks.

2. Microgrid frequency dependent modeling

The hierarchical structure of the proposed EMS for a typical microgrid consisting of n dispatchable VSI-based DG units and some non-dispatchable RES units is depicted in Fig. 1.

In the proposed hierarchical EMS, in the islanded mode, the most important control functions are accomplished by means of the MGCC [29]. The MGCC is in charge to ensure the optimal operation of the microgrid from technical, economic and environmental viewpoints. The MGCC control functions can be achieved through readjustment of the microgrid reference values and are mainly taken place in the line with the DSO operational objectives [30].

The primary control function is performed in a distributed and automatic way while the secondary control functions are usually implemented in a centralized manner [30]. The primary control reserves are supplied using the droop controllers in proportion to the microgrid frequency excursion. In fact, the primary control reserves play a significant role in restricting the frequency excursions and maintaining a stable balance between the microgrid generations and demands. The important note that highlights the emphasis of the primary reserve scheduling is the extreme interdependency to system frequency as a feedback signal to the droop controller which reduces its scheduling degree of freedom comparing to the secondary control reserves [31]. Secondary control reserves mainly rely on the power capacity and ramp-rates of the DG units and can be dispatched among available DG units in accordance to their marginal cost and/or relative emission production. In the following the frequency dependent performances of the microgrid components are formulated accurately.

2.1. VSI-based DG units

The detailed block-diagram of a droop-controlled VSI-based DG unit in the steady-state is illustrated in Fig. 2. The control functions

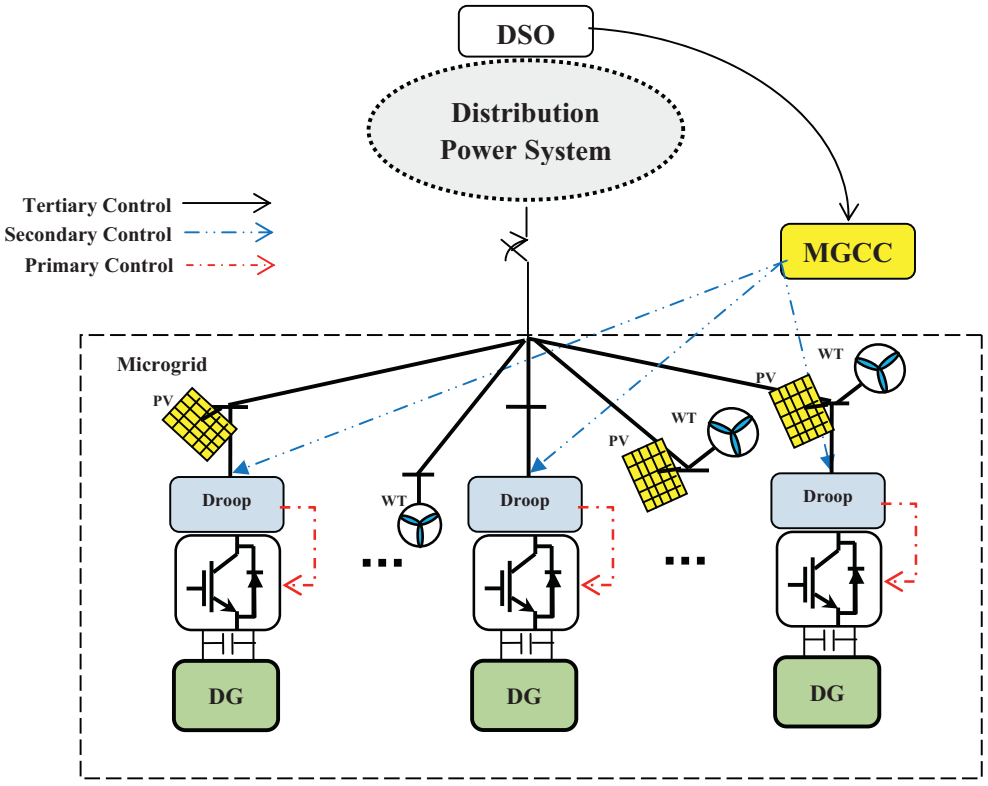

Fig. 1. Hierarchical frequency control structure of a microgrid.

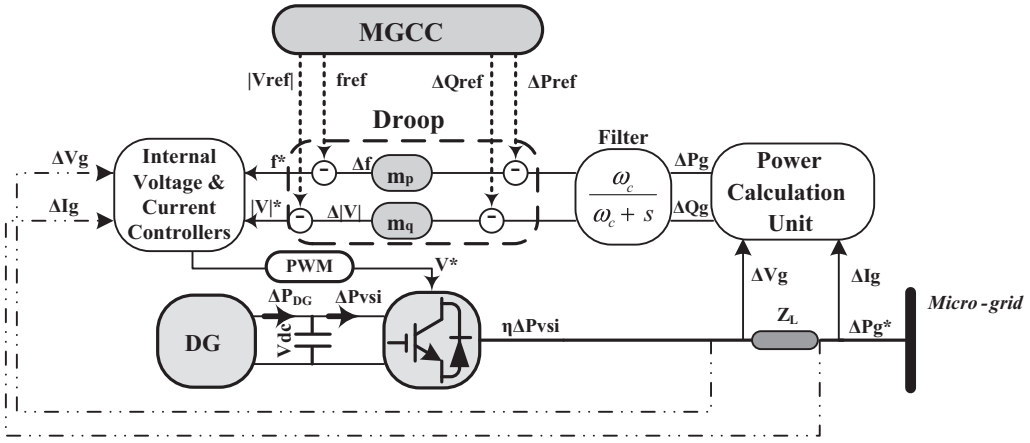

Fig. 2. The steady-state block-diagram of a droop controlled VSI-based DG unit frequency control hierarchical structure.

corresponding to the internal voltage and current controllers have been neglected in the steady-state. Worth to be noted, it is assumed that the microgrid is in the steady-state and all the transients and oscillating modes have been died down.

2.1.1. Primary control level

Microgrid frequency excursion may occur due to the active power variations which stem from the randomly load fluctuations or WT and PV power output deviations. In response to the power variations the committed VSI-based DG units adjust their active power outputs using the droop control method. Eq. (1) describes the performance of the VSI-based DG units in order to maintain the microgrid active power balance.

$$\sum_{i=1}^{Ng}\Delta P^{s}_{i,l,h}=\Delta P^{s}_{L,l,h}-\sum_{w=1}^{Nw}\Delta P^{s}_{w,l,h}-\sum_{v=1}^{Nv}\Delta P^{s}_{v,l,h}+D^{s}_{L,l,h}\cdot\Delta f^{s}_{l,h}-\sum_{d=1}^{Nd}\Delta P^{s}_{d,l,h}-\mathrm{LSH}^{s}_{l,h} \tag{1}$$

To describe the control function of the droop control in the primary level, according to Fig. 2, whenever the microgrid active power balance is deviated as much as ΔP_g, consequently the output voltage and current of the VSI are changed from their scheduled values within ΔV_g and ΔI_g, respectively. Instantly the deviate active power is calculated and its average value is filtered to be used by means of the P–f droop controller. The droop control automatically adjusts the VSI frequency. After regulating the amplitude and the angle of the VSI voltage phasor using the internal voltage and current controllers, Pulse Width Modulation (PWM) unit modifies the VSI switching algorithm such that the desired active power output, i.e. ΔP_{vsi} is generated. In this step, the VSI absorbs the desired active power from the primary source of the DG unit within ΔP_{DG}. It can be assumed that in the steady-state, the primary source is able to supply the VSI active power demands properly. Finally, the generated active power is injected to the microgrid within ΔP^{*}_{g}. According to Fig. 2, the comprehensive static and dynamic performances of the droop controlled VSI can be formulated as follows in Eq. (2):

$$m_{p,i}\cdot\left(\frac{\Delta P^{s}_{i,l,h}}{\frac{s}{\omega_{c,i}}+1}-\Delta P^{s}_{\mathrm{ref},i,l,h}\right)=u^{l}_{i,h}\cdot\left(\Delta f^{s}_{\mathrm{ref},l,h}-\Delta f^{s}_{l,h}\right)\quad l=\mathrm{pri} \tag{2}$$

Where s and $\omega_{c,i}$ describe the Laplace operator and the cut-off frequency of the i-th VSI's low-pass filter, respectively. Eq. (2) can be transformed from the Laplace to the time domain as follows in Eq. (3):

$$\frac{1}{\omega_{c,i}\cdot m_{p,i}}\frac{d(\Delta f^{s}_{l,h}\cdot u^{l}_{i,h})}{dt}=\Delta P^{s}_{\mathrm{ref},i,l,h}-\Delta P^{s}_{i,l,h}-\frac{1}{m_{p,i}}(\Delta f^{s}_{l,h}-\Delta f^{s}_{\mathrm{ref},l,h})\cdot u^{l}_{i,h},\ l=\mathrm{pri} \tag{3}$$

Notably, the reference values corresponding to the DG unit active power set-points and the microgrid reference frequency can be only adjusted by means of the MGCC. On the other hand, since in the primary control level, the control functions are accomplished instantaneously in a few seconds, hence the MGCC has not enough time to change the reference values. Likewise, the commitment states of the DG units are remained unchanged during the primary control level. Eqs. (4)–(6) characterizing that during the primary control level, the reference values as well as the commitment states of the DG units equal to their scheduled values.

$$P^{s}_{\mathrm{ref},i,l,h}\Big|_{l=\mathrm{pri}}=P_{\mathrm{ref},i,h} \tag{4}$$

$$f^{s}_{\mathrm{ref},l,h}\Big|_{l=\mathrm{pri}}=f_{\mathrm{ref},h}=f_{\mathrm{ref}} \tag{5}$$

$$u^{l}_{i,h}\Big|_{l=\mathrm{pri}}=u_{i,h} \tag{6}$$

Thus, the complete frequency control performance of the proposed droop controlled VSI-based DG unit during the primary control level can be explained by Eq. (7):

$$\frac{-1}{\omega_{c,i}\cdot m_{p,i}}\frac{d(\Delta f^{s}_{l,h}\cdot u^{l}_{i,h})}{dt}=\Delta P^{s}_{i,l,h}+\frac{1}{m_{p,i}}\Delta f^{s}_{l,h}\cdot u^{l}_{i,h},\quad l=\mathrm{pri} \tag{7}$$

Apart from the first few seconds of the primary control level, it can be assumed that the transients and the oscillating modes are negligible, i.e. according to Eq. (8), the dynamic control function can be neglected.

$$\frac{d\Delta f^{s}_{l,h}}{dt}\approx 0,\ l=\mathrm{pri} \tag{8}$$

Therefore, Owing to Eq. (8), Eq. (9) can be simply concluded from Eq. (7):

$$\Delta P^{s}_{i,l,h}=-\frac{1}{m_{p,i}}\Delta f^{s}_{l,h}\cdot u^{l}_{i,h},\ l=\mathrm{pri} \tag{9}$$

The static frequency control function of the droop controlled VSI-based DG unit can be expressed according to Eq. (9). To describe the dynamic frequency control function of the droop controlled VSI-based DG unit during the first few seconds, the control function corresponding to the static modeling can be disregarded, therefore Eq. (7) can be simplified as illustrated by Eq. (10):

$$\frac{1}{\omega_{c,i}\cdot m_{p,i}}\frac{d(\Delta f^{s}_{l,h}\cdot u^{l}_{i,h})}{dt}=-\Delta P^{s}_{i,l,h},\ l=\text{pri} \tag{10}$$

Since the microgrid reference frequency equals to the scheduled value during the primary control level, Eq. (11) can be concluded:

$$\frac{d(\Delta f^{s}_{l,h})}{dt}=\frac{d(f^{s}_{l,h}-f^{s}_{\text{ref},l,h})}{dt}=\frac{df^{s}_{l,h}}{dt},\ l=\text{pri} \tag{11}$$

According to Eqs. (10) and (11), (12) clearly represents the dynamic frequency control function of the droop controlled VSI-based DG unit.

$$\frac{1}{\omega_{c,i}\cdot m_{p,i}}\frac{df^{s}_{l,h}}{dt}u^{l}_{i,h}=-\Delta P^{s}_{i,l,h},\ l=\text{pri} \tag{12}$$

It is worth mentioning that the dynamic behavior of a synchronous generator (SG) can be expressed according to Eq. (13) [32,33]:

$$\frac{2H_{S,i}}{f_{\text{ref}}}\frac{df^{s}_{l,h}\cdot u^{l}_{i,h}}{dt}=-\Delta P^{s}_{sg,i,l,h},\ l=\text{pri} \tag{13}$$

where H_S and ΔP_{sg} denote the synchronous inertia and active power deviation of the i-th SG. By simple comparison of Eqs. (10) and (13), it can be concluded that the dynamic behavior of a VSI-based DG unit is dual to an equivalent SG with the nominal power rating equal to P_{rated}. As a contribution of this paper, inspired from Eq. (13), it is proposed to define a virtual inertia (H_V) for the droop controlled VSI-based DG unit as described by Eq. (14):

$$2H_{V,i}=\frac{1}{\omega_{c,i}\cdot m_{p,i}} \tag{14}$$

The virtual inertia concept represents the required time during which the primary source supplies the VSI electrical power demands. As a result, considering to Eqs. (10) and (14), Rate of Change of Frequency (ROCOF) corresponding to i-th VSI with the rated power (P_{rated}) can be calculated using Eq. (15):

$$\text{ROCOF}^{s}_{i,h}\cdot u^{l}_{i,h}=\frac{df^{s}_{l,h}}{dt}\cdot u^{l}_{i,h}=-\frac{f_{\text{ref}}\cdot\Delta P^{s}_{i,l,h}}{2H_{V,i}\cdot P_{\text{rated},i}},\ l=\text{pri} \tag{15}$$

Eq. (15) can also be calculated for the whole microgrid as follows in Eq. (16):

$$\text{ROCOF}^{s}_{\text{MG},h}=-\left(\frac{f_{\text{ref}}\sum_{i=1}^{\text{Ng}}\Delta P^{s}_{i,l,h}}{\sum_{i=1}^{\text{Ng}}2H_{V,i}\cdot P_{\text{rated},i}\cdot u^{l}_{i,h}}\right),\ l=\text{pri} \tag{16}$$

2.1.2. Secondary control level

During the primary control level, the VSI-based DG units alleviate the frequency excursions by adjusting their active power outputs in proportion to the frequency excursions. However, due to inherent errors of the droop controllers, the microgrid frequency may be stabilizes at a value which may be distinctive to the reference frequency. In such cases, the MGCC can restore the frequency to its reference value by readjustment the active power set-points of dispatchable DG units and also the demand response resources. Worth mentioning that, the restoration function should be carried out subject to the microgrid economic and environmental targets. According to Fig. 2, the MGCC supervisory control function during the secondary level can be formulated by Eq. (17):

$$P^{s}_{i,l,h}-P_{i,h}=u^{l}_{i,h}\cdot\left[P^{s}_{\text{ref},i,l,h}-P_{\text{ref},i,h}-\frac{1}{m_{p,i}}(f^{s}_{l,h}-f_{\text{ref}})\right],\ l=\text{sec} \tag{17}$$

Obviously, according to Eq. (18), the scheduled reference power set-point and the dispatched active power output of the i-th VSI-based DG unit are equal:

$$P_{i,h}\cdot u_{i,h}=P_{\text{ref},i,h} \tag{18}$$

Therefore, Eq. (17) can be simplified according to Eq. (18), as follows in Eq. (19):

$$P^{s}_{i,l,h}=u^{l}_{i,h}\cdot\left[P^{s}_{\text{ref},i,l,h}-\frac{1}{m_{p,i}}\left(f^{s}_{l,h}-f_{\text{ref}}\right)\right],\ l=\text{sec} \tag{19}$$

Finally, using Eqs. (1), (9) and (19), the microgrid primary and secondary frequency excursion can be easily calculated as follows in Eqs. (20) and (21), respectively:

$$\Delta f^{s}_{l,h}\Big|_{l=\text{pri}}=-\frac{\Delta P^{s}_{L,l,h}-\sum_{w=1}^{\text{Nw}}\Delta P^{s}_{w,l,h}-\sum_{v=1}^{\text{Nv}}\Delta P^{s}_{v,l,h}-\text{LSH}^{s}_{l,h}(l,h)}{D^{s}_{L,l,h}+\sum_{i=1}^{\text{Ng}}\frac{1}{m_{p,i}}\cdot u^{l}_{i,h}},\ l=\text{pri} \tag{20}$$

$$\Delta f^{s}_{l,h}\Big|_{l=\text{sec}}=\frac{\sum_{i=1}^{\text{Ng}}[P^{s}_{\text{ref},i\cdot l,h}-P^{s}_{i,l,h}]}{D^{s}_{L,l,h}+\sum_{i=1}^{\text{Ng}}\frac{1}{m_{p,i}}\cdot u^{l}_{i,h}},\ l=\text{sec} \tag{21}$$

It is clear that if the secondary frequency is controlled at exactly the reference value, therefore it the MGCC has to adjust the reference active power set-point according to Eq. (22):

$$\begin{aligned}&\Delta f^{s}_{l,h}\Big|_{l=\text{sec}}=0;\\&P^{s}_{\text{ref},i\cdot l,h}\Big|_{l=\text{sec}}=P^{s}_{i,l,h}\Big|_{l=\text{sec}}\cdot u^{l}_{i,h}\Big|_{l=\text{sec}}\end{aligned} \tag{22}$$

2.2. Renewable energy sources

Wind Turbine (WT) and Photovoltaic (PV) unit power outputs are inherently intermittent. The corresponding uncertainties of the WT and PV units are modeled by generating some random scenarios using the MCS strategy and in accordance to the corresponding Probability Density Functions (PDFs) [34]. Worth to mentioned, due to uncontrollable nature of the WT and PV units, it is assumed that they are not participated into the microgrid frequency management approach. Hence, the dispatchable DG units are responsible to compensate the power variations stem from the random power outputs of the RES units [35]. The uncertainty associated with the PV unit power output is modeled using the normal PDF as illustrated in Fig. 3. Depending on the desired accuracy, the PDF is divided to a number of discrete intervals with different probability levels [36]. In this paper, the PDF is divided into seven intervals. Each discretized interval with width of σ corresponds to a specified error value with respect to the forecasted power generation of the PV units. To model each probability level associated with the PV stochastic power output, the RWM strategy is

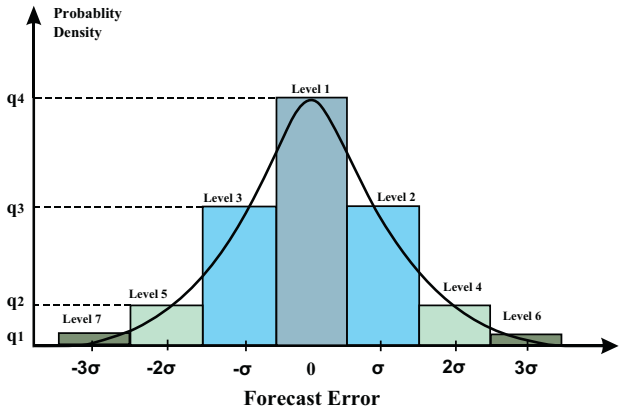

Fig. 3. Discretized probability distribution function corresponding to the considered forecast errors.

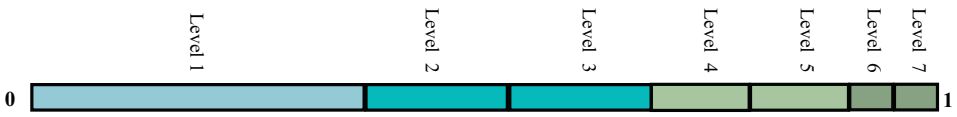

Fig. 4. Roulette Wheel Mechanism for normalized probabilities of the considered forecast errors.

employed as depicted in Fig. 4 [37]. Each interval throughout the roulette wheel indicates a specific forecasting error corresponding to the PV power output. The probabilities of the intervals on the roulette wheel are normalized such that their summation equals to unity. To generate a scenario corresponding to each forecast error of the PV power output, first using the MCS a random number in the range of [0–1] is generated. Each interval on the roulette wheel in which the generated random number falls is corresponding to a scenario of the PV output power.

Statistically, Weibull PDF is rather employed to characterize the uncertainty related to the WT units. Therefore, the divided Weibull PDF is usually used in order to model the stochastic power outputs of the WT units. The general Weibull PDF of wind speed including the three scale (c), shape (K) and location (v_0) parameters can be formulated as follows in Eq. (23) [36]:

$$\mathrm{PDF}(v) = \frac{K}{c}\left(\frac{v - v_0}{c}\right)^{K-1} \cdot \exp\left[-\left(\frac{v - v_0}{c}\right)^{K}\right] \tag{23}$$

Besides, the relationship between the wind speed and WT active power generation can be described by Eq. (24) [38]:

$$P_w(v) = P_{\mathrm{WT}} \times \begin{cases} 0 & 0 \leqslant v \leqslant v_i \\ a + b v^3 & v_i \leqslant v \leqslant v_r \\ 1 & v_r \leqslant v \leqslant v_o \\ 0 & v \geqslant v_o \end{cases} \tag{24}$$

where v_r, v_i and v_o indicate the rated wind speed, cut-in speed of wind and cut-out speed of wind, respectively. a and b are parameters which are given as the following [38]:

$$a = \frac{v_i^3}{v_i^3 - v_r^3};\ b = \frac{1}{v_r^3 - v_i^3} \tag{25}$$

To generate the associated scenarios of the WT power output errors, the Weibull PDF should also be divided into some discrete intervals and the same procedure using the MCS and RWM strategies should be employed.

2.3. Electrical loads

Microgrid loads can also take part into the frequency control procedure on the basis of their natural elasticity to the system frequency or in the light of scheduling the demand response programs. In the primary control level, due to the time limitation of this control level, it seems that without any advanced metering infrastructure it may not possible to schedule the microgrid loads for participating into the primary frequency control [39]. Recently it has been proposed that for some certain loads like thermostatic controlled loads equipped with frequency aware controllers, the primary frequency regulation services can be provided from the end-user consumers [40]. However, due to lower level of the energy consumption in the microgrids, providing primary frequency control services from end-user consumers not only may not be effective in terms of technical aspects but also may disrupt the relative comfort of the consumers. As a result, it is not possible to schedule the electrical loads for provision of the primary frequency control. However, on the basis of the natural and uncontrollable elasticity of the electrical loads to the system frequency, in this paper, it is considered that electrical loads can change their power consumption in response to the microgrid frequency excursions. Clearly, the participation of the loads according to their natural tendency can help the VSI-based DG units managing the microgrid frequency with lower fuel cost and emission production. Eq. (26) presents the load-frequency dependency modeling of the electrical loads in both primary and secondary control levels:

$$P^s_{L,l,h,f} = P_{L,h} + D^s_{L,l,h} \cdot \Delta f^s_{l,h} \tag{26}$$

where $D^s_{L,l,h}$ represents the elasticity of the microgrid electrical loads to the frequency which can be determined easily according to Eq. (27) in scenario s, control level l and hour h:

$$D^s_{L,l,h} = \frac{\partial P^s_{L,l,h,f}}{\partial f^s_{l,h}} \approx \frac{P^s_{L,l,h}}{f_{\mathrm{ref}}} \tag{27}$$

Obviously, the microgrid loads have inherently probabilistic behavior that requires modeling the associated uncertainty. In this paper, the uncertainty of the electrical load consumption is modeled using the same approach proposed to model the intermittency of the RES units. The load forecast error is modeled using the normal discretized PDF as represented in Fig. 3. An analogous approach based on the MCS and RWM is performed to generate the random scenarios corresponding to the load forecast error. Thus, according to the above discussion, each scenario is a combination of the different forecast errors corresponding to the WT, PV units as well as the load consumption. Each scenario has a normalized probability (π_s), associated to the selected intervals in the roulette wheel for the WT, PV and load forecast errors. The final structure of the s-th scenario at hour h can be described by Eq. (28):

$$\left[P^s_{w,l,h,1}, \ldots, P^s_{w,l,h,\mathrm{Nw}}, P^s_{v,l,h,1}, \ldots, P^s_{v,l,h,\mathrm{Nv}}, P^s_{L,l,h}\right],\quad s = 1,2,\ldots,\mathrm{Ns};\ h = 1,2,\ldots,\mathrm{Nh} \tag{28}$$

After generating the scenarios, to attain a trade-off between the computational efficiency and the solution accuracy, a proper scenario reduction algorithm is applied to the generate scenarios to remove the low probable and similar scenarios [41]. Each of remained scenarios should be solved deterministically owing to its probability. Finally, to find out the expected result of the problem and simplification the solution interpretation, obtained solutions from the reduced scenarios are aggregated according to their normalized probability.

2.4. Demand response resources

Together with DG units, DRPs can also be considered as the main components in the microgrids. In other words, to attain an optimal operation, the DR is one of the most commodious resources [42,43]. Accordingly, in a smart microgrid, coordinated control of the DR resources can considerably promote the provision of the frequency control ancillary services and improving the microgrid reliability. Generally, DR programs are classified into the price based and incentive based ones. In this paper, based on the dispatchability and compatibility characteristics of the incentive based programs, the Demand Bidding and Ancillary Service programs are proposed to be exploited into the microgrid fre-

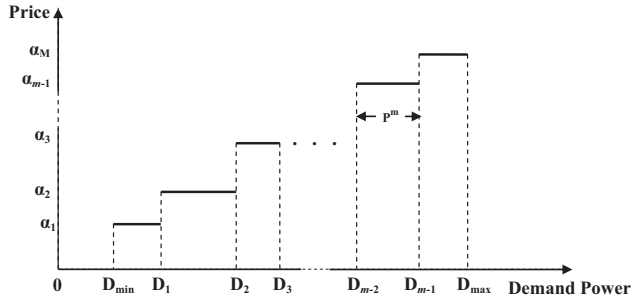

Fig. 5. The proposed step-wise demand response price-demand curve.

quency management procedure [43–46]. For this purpose, DRPs are employed to submit their demand reduction offers to the MGCC. While the offers are accepted, the DRPs are called to reduce the suggested demand. Obviously, the proposed DR programs are incorporated into the secondary control level and also can be utilized for energy provision. In this paper, the proposed DR programs are modeled using a step-wise price-demand curve as depicted in Fig. 5.

D_{max} and D_{min} are sum of all deployed load curtailments and minimum acceptable load reduction that each DRP can carry it out, respectively. α_m and $P^m_{d,h}$ are offered price and reduced demand level of mth step, respectively. $P_{d,h}$ is total hourly curtailed load by means of d-th DRP at hour h. Eqs. (29)–(32) describing the mathematical modeling of the proposed DR programs as follows:

$$D_{\min,d} \leqslant P^m_{d,h} \leqslant D_m, \ \forall m = 1 \tag{29}$$

$$0 \leqslant P^m_{d,h} \leqslant D_m - D_{m-1}, \ \forall m = 2,3,\ldots,M \tag{30}$$

$$P_{d,h} = \sum_{m=1}^{M} P^m_{d,h} \tag{31}$$

$$D_{\min,d} \leqslant P_{d,h} \leqslant D_{\max,d} \tag{32}$$

3. Problem formulation

To ensure the reliable management of the microgrid frequency security, it is aimed that energy and reserve resources are scheduled such that the microgrid overall operational aspects are satisfied. In other words, the MGCC should control the microgrid frequency such that the corresponding cost and emission levels are justified reasonably. Hence, in this paper, it is aimed to manage the microgrid frequency such that the operational goals of the microgrid are managed into the secure ranges. In this regards, the overall operational aspects of the microgrid are formulated using four indices as the following.

3.1. Microgrid operational indices

3.1.1. Total Frequency Excursion index (TFE)

The microgrid hourly frequency excursion is employed as a technical index to evaluate the static frequency security of the microgrid. Eq. (33) formulates the proposed TEF index:

$$\text{TEF} = \sum_{s=1}^{\text{Ns}} \sum_{h=1}^{\text{Nh}} \sum_{l} \pi_s \cdot |\Delta f^s_{l,h}| \tag{33}$$

To ensure the microgrid static frequency security is procured reliably, the MGCC should manage the frequency excursion index in a secure range according to Eq. (34).

$$|\Delta f^s_{l,h}| \leqslant \Delta f^{\max}_l, \quad l = \text{pri}, \text{sec} \tag{34}$$

where $\Delta f^{\max}_l$ represent the maximum allowable range corresponding to the microgrid frequency excursion in control level l.

3.1.2. Rate of Change of Frequency index (RCF)

To assess the dynamic frequency security of the microgrid the RCF index is formulated. RCF index appraises both the rate of change of DG frequency and rate of change of the whole microgrid frequency. Eq. (35) represents the proposed RCF index:

$$\text{RCF} = \sum_{s=1}^{\text{Ns}} \sum_{h=1}^{\text{Nh}} \pi_s \cdot \left[\left| \text{ROCOF}^s_{\text{MG},h} \right| + \sum_{i=1}^{\text{Ng}} \left| \text{ROCOF}^s_{i,h} \right| \right] \tag{35}$$

Likewise, to ensure the microgrid dynamic frequency security, the MGCC should manage the rates of change of DG as well as the microgrid frequency in secure ranges according to Eqs. (36) and (37), respectively.

$$|\text{ROCOF}^s_{i,h}| \leqslant \text{ROCOF}^{\max}_i \cdot u^l_{i,h}, \quad l = \text{pri} \tag{36}$$

$$|\text{ROCOF}^s_{\text{MG},h}| \leqslant \text{ROCOF}^{\max}_{\text{MG}} \tag{37}$$

where $\text{ROCOF}^{\max}_i$ and $\text{ROCOF}^{\max}_{\text{MG}}$ represent the maximum allowable ranges corresponding to rate of change of i-th DG unit frequency and the rate of change of the whole microgrid frequency, respectively.

3.1.3. Total Operation Cost index (TOC)

The microgrid day-ahead operation costs can be assessed using the proposed TOC index as follows in Eq. (38):

$$\text{TOC} = \sum_{h=1}^{\text{Nh}} \left(\begin{array}{l} \sum_{i=1}^{\text{Ng}} [a_i \cdot u_{i,h} + b_i \cdot P_{i,h}] + \rho_w \cdot \sum_{w=1}^{\text{Nw}} P_{w,h} + \rho_v \cdot \sum_{v=1}^{\text{Nv}} P_{v,h} \\ + \sum_{d=1}^{\text{Nd}} \sum_{m=1}^{M} \alpha^E_{d,m} \cdot P^m_{d,h} \\ + \sum_{i=1}^{\text{Ng}} \sum_{l} \sum_{ud} \rho^R_{i,l,ud} \cdot R_{i,l,ud,h} + \sum_{d=1}^{\text{Nd}} \sum_{l=\text{sec}} \sum_{ud} \alpha^R_{d,l,ud} \cdot R_{d,l,ud,h} \\ + \sum_{s=1}^{\text{Ns}} \sum_{l} \pi_s \left(\begin{array}{l} \sum_{i=1}^{\text{Ng}} [a_i \cdot u^l_{i,h} + b_i \cdot P^s_{i,l,h}] + \rho_w \cdot \sum_{w=1}^{\text{Nw}} P^s_{w\cdot l\cdot h} \\ + \rho_v \cdot \sum_{v=1}^{\text{Nv}} P^s_{v\cdot l\cdot h} + \sum_{d=1}^{\text{Nd}} \sum_{m=1}^{M} \alpha^E_{d,m} \cdot P^{s,m}_{d,l,h} \end{array} \right) \\ + \text{voll} \cdot \text{ELNS}_h \end{array} \right) \tag{38}$$

The term ELNS shows expected load not supplied and can be calculated as follows in Eq. (39):

$$\text{ELNS}_h = \sum_{s=1}^{\text{Ns}} \sum_{l} \pi_s \cdot \text{LSH}^s_{l,h} \tag{39}$$

The MGCC should manage the microgrid frequency considering to the reliable operational cost requirements of the microgrid. Therefore, the TOC index should also be managed in a secure range as follows in Eq. (40):

$$\text{TOC} \leqslant \text{TOC}_{\max} \tag{40}$$

where $\text{TOC}_{\max}$ denotes the maximum allowable range corresponding to the microgrid day-ahead operational cost.

3.1.4. Total Operation Emission index (TOE)

The microgrid hourly CO_2 production is formulated as the environmental index which is described according to Eq. (41):

$$\text{TOE} = \sum_{h=1}^{\text{Nh}} \left[\sum_{i=1}^{\text{Ng}} E^g_i \cdot P_{i,h} + \sum_{s=1}^{\text{Ns}} \sum_{i=1}^{\text{Ng}} \sum_{l} \pi_s \cdot E^g_i \cdot P^s_{i,l,h} \right] \tag{41}$$

Similarly, as follows in Eq. (42), the MGCC should also manage the proposed environmental index in accordance to the microgrid emission policy.

$$\mathrm{TOE} \leqslant \mathrm{TOE}_{\max} \tag{42}$$

where $\mathrm{TOE}_{\max}$ explains the maximum allowable range corresponding to the microgrid day-ahead operational emission production.

3.2. Objective function

As mentioned previously, in the islanded microgrids, the frequency security has superior importance with respect to the economic goals. However, the MGCC should provide the security with acceptable operation cost and emission such that the security procurement is justified. Hence, in this paper, the main objective function is constructed based on the MG frequency profile which is a combination of static and dynamic frequency indices. Eq. (43) explains the general methodology of the paper. J is the proposed frequency dependent objective function which constructed based on the TEF and RCF operational indices. Worth mentioning that $\mathrm{TOC}_{\max}$ and $\mathrm{TOE}_{\max}$ are determined by means of the MGCC in the line of the EMS operational policies.

$$\min J = \min \left\{ \left[\sum_{s=1}^{\mathrm{Ns}} \sum_{h=1}^{\mathrm{Nh}} \sum_{l} \pi_s \cdot \left| \Delta f_{l,h}^{s} \right| \right] + \mu \cdot \sum_{s=1}^{\mathrm{Ns}} \sum_{h=1}^{\mathrm{Nh}} \pi_s \cdot \left[\left| \mathrm{ROCOF}_{\mathrm{MG},h}^{s} \right| + \sum_{i=1}^{\mathrm{Ng}} \left| \mathrm{ROCOF}_{i,h}^{s} \right| \right] \right\} \tag{43}$$

$s \cdot t \cdot$

$\mathrm{TOC} \leqslant \mathrm{TOC}_{\max}$;

$\mathrm{TOE} \leqslant \mathrm{TOE}_{\max}$.

The paper is aimed to schedule the energy and reserve resources such that the staric and dynamic frequency excursions are minimized and meanwhile the economic and environmental goals are assured.

3.3. Operational constraints

The developed optimization framework should be solved subject to several constraints restricting the microgrid frequency management. In the following, related constraints are expressed.

3.3.1. Frequency dependent constraints

As mentioned, microgrid frequency is heavily dependent to the variations of the WT and PV unit power outputs as well as the load demand fluctuations. The frequency dependent performances of the microgrid components are formulated thoroughly using Eqs. (1)–(22). Furthermore, the MGCC is in charge to provide the proposed microgrid fourfold operational indices securely as illustrated by Eqs. (33)–(42).

3.3.2. DER power and reserve constraints

The constraints described by Eqs. (44)–(49) are employed to explain the physical limitations of the DER unit active power outputs, DG unit reference active power set-points and scheduled reserve resources.

$$P_i^{\min} \cdot u_{i,h} \leqslant P_{i,h} \leqslant P_i^{\max} \cdot u_{i,h} \tag{44}$$

$$P_i^{\min} \cdot u_{i,h}^{l} \leqslant P_{\mathrm{ref},i,l,h}^{s} \leqslant P_i^{\max} \cdot u_{i,h}^{l} \tag{45}$$

$$R_{i,l,ud,h} \geqslant P_{\mathrm{ref},i,l,h}^{s} - P_{i,h},\ ud = up \tag{46}$$

$$R_{i,l,ud,h} \geqslant P_{i,h} - P_{\mathrm{ref},i,l,h}^{s},\ ud = dn \tag{47}$$

$$R_{d,l,ud,h} \geqslant P_{d,l,h}^{s} - P_{d,h},\ ud = dn,\ l = \mathrm{sec} \tag{48}$$

$$R_{d,l,ud,h} \geqslant P_{d,h} - P_{d,l,h}^{s},\ ud = up,\ l = \mathrm{sec} \tag{49}$$

Constraints presented in Eqs. (46) and (47) are used to determine the precise amounts of the scheduled up and down frequency control reserves corresponding to the DG units. It has been assumed in this paper that the precise amounts of the DERs' frequency control reserves in both primary and secondary control levels are determined on the basis of the reference power set-point of the DG units. Similarly, Eqs. (48) and (49) are also used to describe the DR reserve constraints. Other technical limitations of the DG units including ramp up and down restrictions and also the minimum up and down time limits are also considered in the proposed optimization framework.

3.3.3. Hourly power balance

The hourly power balance equations of the microgrid can be represented by Eqs. (50) and (51), respectively:

$$\sum_{i=1}^{\mathrm{Ng}} P_{i,h} + \sum_{w=1}^{\mathrm{Nw}} P_{w,h} + \sum_{v=1}^{\mathrm{Nv}} P_{v,h} + \sum_{d=1}^{\mathrm{Nd}} P_{d,h} = P_{L,h} \tag{50}$$

$$\sum_{i=1}^{\mathrm{Ng}} P_{i,l,h}^{s} + \sum_{w=1}^{\mathrm{Nw}} P_{w,l,h}^{s} + \sum_{v=1}^{\mathrm{Nv}} P_{v,l,h}^{s} + \sum_{d=1}^{\mathrm{Nd}} P_{d,l,h}^{s} = P_{L,l,h}^{s} + D_{L,l,h}^{s} \cdot \Delta f_{l,h}^{s} - \mathrm{LSH}_{l,h}^{s} \tag{51}$$

Eq. (50) describe the hourly power balance of the microgrid in both primary and secondary frequency control levels. Noticeably, DRPs are not participated into the primary control level, therefore, if DRPs are called from the MGCC to provide energy, in the primary control level, they are not authorized to change their power demand as follows in Eq. (52).

$$P_{d,l,h}^{s}\Big|_{l=\mathrm{pri}} = P_{d,h} \tag{52}$$

4. Simulation and numerical results

The developed model is analyzed in two case-studies. In case 1, it is assumed that microgrid frequency security is managed without the DR programs. In case 2, the proposed ancillary service DR programs are taken into account. The MGCC is aimed to restore the secondary frequency at exactly the rated value, i.e. 60 Hz. The operational requirements of the simulated case-studies are listed in Table 1.

The simulations are performed over a modified low-voltage microgrid system which is presented in Fig. 6. The proposed mathematical modeling is examined over a 24 h scheduling time horizon. The microgrid is operated in the islanded mode and contains five inverter-based droop controlled DG units. The droop controlled DG units consist of two Micro-Turbines (MTs), two Fuel Cells (FCs) and a Gas Engine (GE) unit. Additionally, three similar WT and two PV units are also dispersed in the distribution feeders. Besides, two DRPs are considered to offer the end-user consumer load reduction bids to the MGCC. The techno-economic data of the microgrid are taken from [30,47,48] and illustrated in Table 2. The step-wise price-demand curves of the DRPs are shown in Fig. 7. The cost of demand-side reserves are 0.85 and 0.9 cent/kW for DRP1 and DRP2, respectively.

Besides, the hourly forecasted active power outputs of the WTs and PVs and also the hourly load consumption pattern are illustrated in Fig. 8 [30]. The value of the MG lost load (voll) is assumed to be 1000 cent/kW h. In this study, first 1000 scenarios consist of the aggregated load consumption and WT and PV power output uncertainties are generated using the proposed MCS and RWM methodologies. Then by implementing an efficient scenario reduction algorithm, 20 scenarios have been remained. The reduced scenarios have been applied to the proposed MILP optimization model. The aforementioned case studies have been performed on a platform with Intel Core i5-4660 CPU and 8 GB of RAM. The

Table 1
Operational requirements of the simulated case-studies.

Case	TOC_{max} (cent)	TOE_{max} (kg)	Δf_{pri}^{max} (mHz)	$ROCOF_i^{max}$ (Hz/s)	$ROCOF_{MG}^{max}$ (Hz/s)
Case 1 – without DR	500,000	13,500	±300	±0.6	±0.5
Case 2 – with DR	425,000	7500	±300	±0.6	±0.5

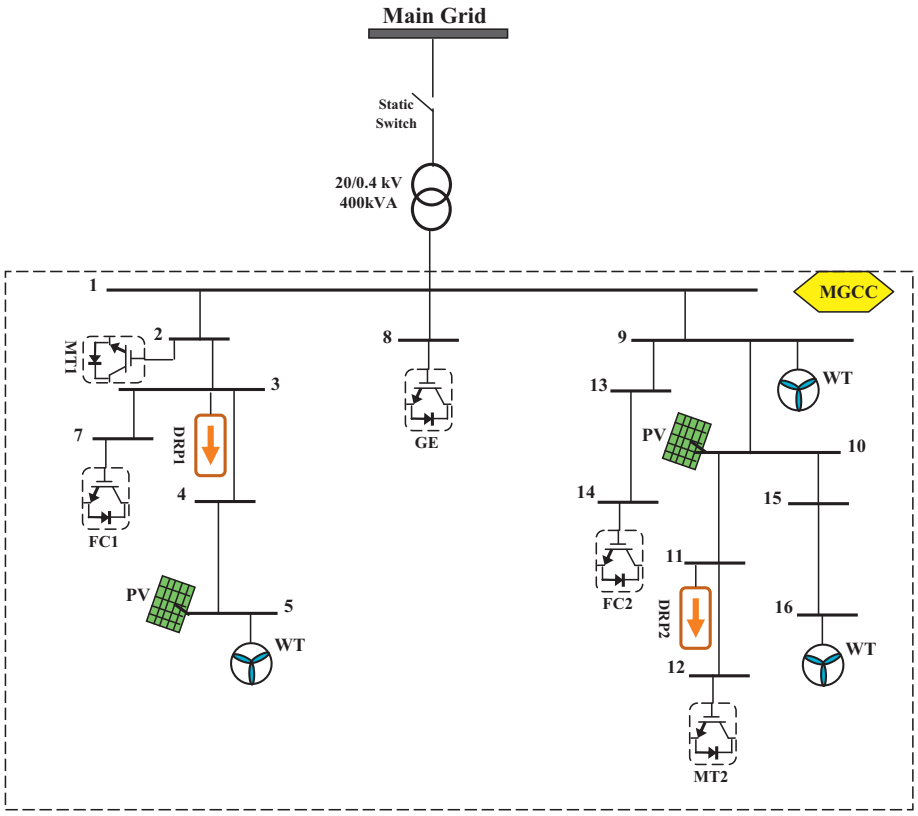

Fig. 6. Microgrid test system.

Table 2
The techno-economic data of the microgrid.

DG	Minimum generation limit (kW)	Maximum generation limit (kW)	Fixed cost (cents/h)	Generation cost (cents/kW h)	Start-up cost (cents)	Shut-down cost (cents)	Primary reserve cost (cents)	Secondary reserve cost (cents)	Droop coefficient (mHz/kW)	Virtual inertia (sec)	Emission rate (kg/kW h)
MT	25	150	85.06	4.37	9	8	6.00	2.10	10.0	6	0.550
FC	20	100	255.18	2.84	16	9	4.00	1.50	15.0	8	0.377
GE	35	200	212.00	3.12	12	8	3.80	1.70	7.5	5	0.890
WT	0	80	0	10.63	–	–	–	–	–	–	–
PV	0	70	0	54.84	–	–	–	–	–	–	–

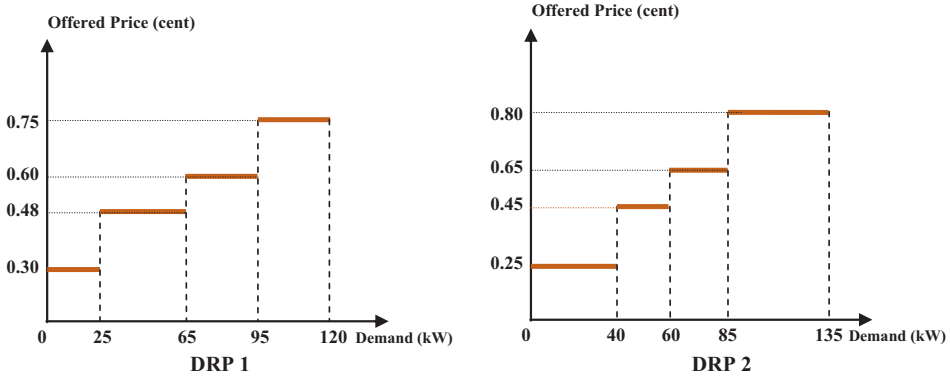

Fig. 7. Offered demand response curves.

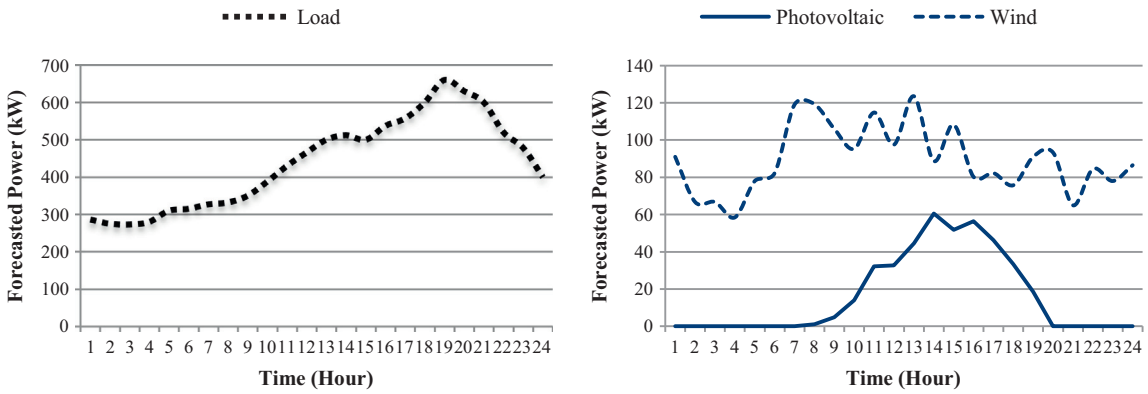

Fig. 8. Hourly forecasted values of the load consumption, WT and PV unit active power outputs.

Table 3
The optimization hourly values of the objective function, TEF and RCF indices with and without DR programs (Optimization results in hour 21 are discussed in-depth.)

Index	Objective function (Hz)		TFE (mHz)		RCF (Hz/s)	
Hour	Case 1	Case 2	Case 1	Case 2	Case 1	Case 2
1	0.219	0.219	75.434	75.434	1.437	1.437
2	0.205	0.205	70.582	70.582	1.345	1.345
3	0.312	0.312	107.630	107.630	2.051	2.051
4	0.176	0.176	60.712	60.712	1.157	1.157
5	0.254	0.254	87.524	87.524	1.670	1.670
6	0.184	0.184	63.494	63.494	1.211	1.211
7	0.200	0.200	68.919	68.919	1.316	1.316
8	0.238	0.238	81.912	81.912	1.561	1.561
9	0.124	0.124	42.605	42.605	0.814	0.814
10	0.293	0.294	100.670	101.140	1.928	1.937
11	0.392	0.392	134.261	134.261	2.576	2.576
12	0.291	0.291	99.973	99.972	1.917	1.917
13	0.373	0.373	127.842	127.842	2.459	2.459
14	0.327	0.327	111.804	111.804	2.151	2.151
15	0.253	0.253	86.933	86.933	1.670	1.670
16	0.149	0.155	51.063	53.183	0.980	1.020
17	0.167	0.181	57.254	62.257	1.099	1.196
18	0.377	0.377	128.759	128.758	2.486	2.486
19	0.214	0.219	73.052	74.917	1.408	1.444
20	0.361	0.361	123.269	123.269	2.377	2.377
21	0.131	**0.383**	44.701	**130.780**	0.862	**2.526**
22	0.322	0.322	110.076	110.076	2.118	2.118
23	0.240	0.240	81.828	81.827	1.571	1.571
24	0.188	0.188	64.493	64.493	1.235	1.235
Total	5.995	6.276	2054.796	2150.334	39.409	41.256

Table 4
The optimization hourly values corresponding to the TOC, TOE and ELNS indices with and without DR programs (Optimization results in hour 21 are discussed in-depth.)

Index	TOC (cents)		TOE (kg)		ELNS (kW h)	
Hour	Case 1	Case 2	Case 1	Case 2	Case 1	Case 2
1	8755.56	8509.13	347.48	319.50	1.06	1.06
2	7185.45	6635.21	365.57	295.37	0.06	0.06
3	7232.18	6680.89	374.85	295.96	0.14	0.14
4	6767.91	5898.50	363.65	192.77	0	0
5	7586.22	6923.16	378.55	289.49	0	0
6	9070.08	8459.20	381.72	292.21	1.50	1.50
7	10875.90	10059.31	354.73	188.12	2.82	2.82
8	8146.25	7806.77	333.47	290.18	0	0
9	8269.56	7444.58	378.82	260.56	0.01	0.01
10	11173.40	9762.96	475.23	275.37	1.14	0.92
11	31661.30	30153.89	521.19	238.40	19.05	19.05
12	16206.30	14879.74	551.73	311.46	3.65	3.65
13	32853.80	31279.82	614.13	339.86	19.06	19.06
14	24974.60	22514.24	655.50	267.20	10.15	10.15
15	32161.10	30764.01	527.63	328.13	15.99	15.99
16	17750.30	14993.11	657.43	295.14	3.18	2.17
17	18516.29	14380.98	658.54	304.09	2.81	0.42
18	45869.59	43051.11	841.30	416.11	29.66	29.66
19	19179.60	15444.64	845.37	416.77	3.98	3.08
20	23502.40	20838.06	843.67	406.44	9.95	9.95
21	104472.10	**60700.05**	931.74	**505.28**	93.64	**52.43**
22	24281.40	21585.46	767.59	363.08	13.87	13.87
23	12076.60	9891.71	710.19	318.86	2.70	2.70
24	8368.44	6941.45	519.85	289.56	0	0
Total	496936.61	415598.05	13,400	7500	234.50	188.76

corresponding developed MILP model is solved using CPLEX as a powerful efficient solver under the GAMS environment [49].

In Table 3, the hourly optimized values of the objective function (J) and the frequency dependent indices, i.e. TFE and RCF have been listed. Table 4 illustrates the hourly optimizations values corresponding to the economic and environmental indices as well as hourly values of the expected load not supplied. Total hierarchical cost and emission levels of the scheduled energy and reserves are broken down in Table 5.

As it is clear from Tables 3 and 4, in case 2, in which the ancillary service DR program has been taken into consideration, the hourly values of the TOC, TOE and ELNS indices have been reduced significantly. However, the optimized amounts corresponding to the frequency dependent indices, i.e. TEF and RCF have been increased slightly. As a result, the objective function has been also increased from 5.995 to 6.276 Hz. It is because of that the DR programs have not been participated in the primary frequency control level. On the other hand, participation of the DRPs in providing the microgrid energy requirements leads the expensive DG units such FCs not to commit in some hours. This makes the primary frequency excursions and the rate of change of microgrid frequency become larger due to lower amounts of online droop controllers and less committed virtual inertias. The greater amounts of the TEF and RCF indices verify the claim. As a result, the remained committed DG units have to generate more active power in the primary control level to cope with the greater primary frequency excursions and the ROCOF. Hence, the scheduled primary control reserves in case 2 have been procured more costly comparing to case 1. As presented in Table 5, the daily cost of the scheduled primary control reserves has been increased from 10779.30 cents in case 1 to 11462.58 cents in case 2. However, the costs of the provided energy and scheduled secondary control reserves have been decreased in case 2, where the DR programs are incorporated. Moreover, due to the participation of the DRPs in providing the energy and secondary control reserves, the costs associated to the deployment of the primary and secondary control reserves have been decreased greatly. Notably, despite the greater values of the primary frequency excursions, due to lower values of the

Table 5
The break-down of the hierarchical cost and emission levels corresponding to the scheduled energy and reserve resources.

Case	Energy cost (cents)		Scheduled reserve cost (cents)				Deployed reserve cost (cents)			
	DG	DR	Primary		Secondary		Primary		Secondary	
			DG	DR	DG	DR	DG	DR	DG	DR
Case 1	48801.46	–	10779.30	–	5087.84	–	50575.33	–	50919.89	–
Case 2	36910.34	966.05	11462.58	0	4464.53	1198.78	38848.23	0	35336.66	1371.538

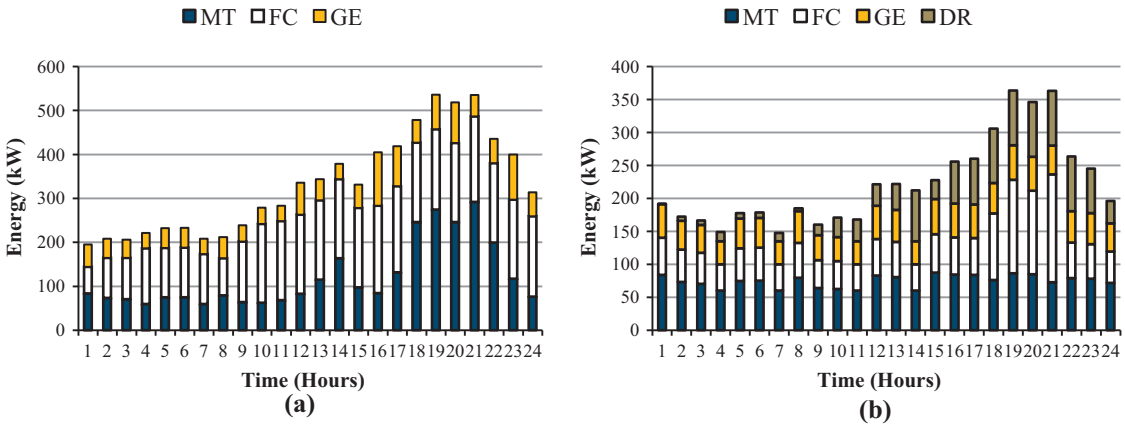

Fig. 9. Provided energy in case 1 (a) and case 2 (b).

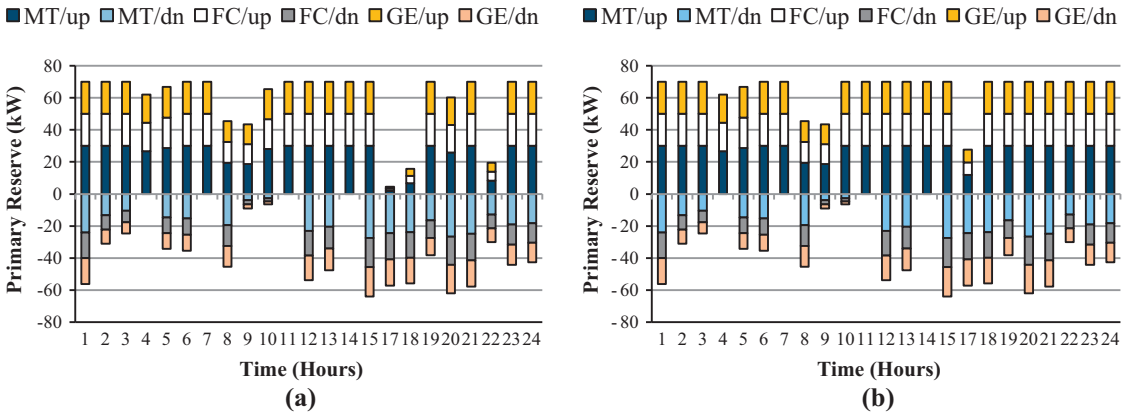

Fig. 10. Scheduled primary control reserves in case 1 (a) and case 2 (b).

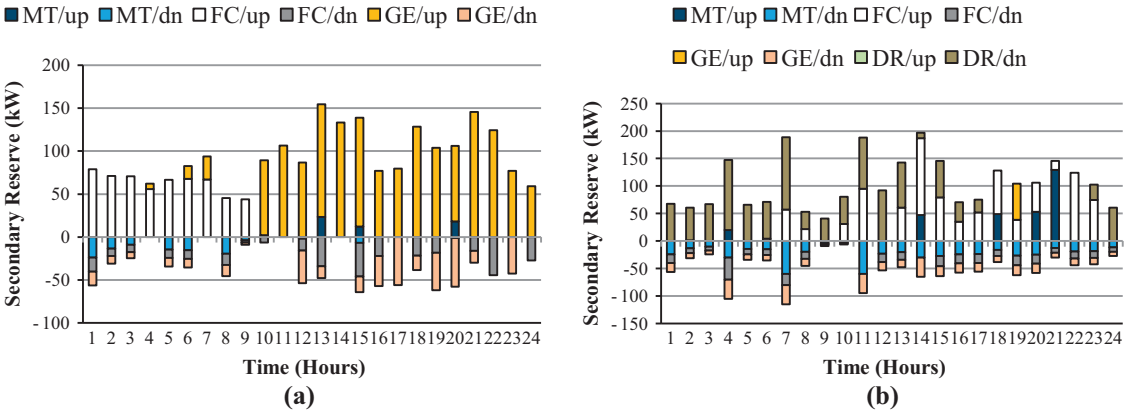

Fig. 11. Scheduled secondary control reserves in case 1 (a) and case 2 (b).

Table 6
Operational characteristics of scenarios 2 and 15 in hour 12 in cases 1 and 2.

Scenario	π_s	ΔP_w (kW)	ΔP_v (kW)	ΔP_L (kW)	D_L (kW/Hz)	LSH (kW h)	Δf_{pri} (mHz)	$ROCOF_{MG}$ (Hz/s)	Expected operation cost (cents)		Expected emission (kg)	
									Case 1	Case 2	Case 1	Case 2
2	0.209	23.4	−6.99	93.2	9.32	6.76	−147.12	−0.477	11242.46	10131.31	467.56	354.72
15	0.025	23.4	6.99	−23.3	7.38	0.00	+113.26	+0.365	3629.67	2787.58	243.40	158.46

Table 7
Optimization results in hour 12 during scenarios 2 and 15.

Case	Case 1: Without DR					Case 2: With DR					
DER	MT1	MT2	FC1	FC2	GE	MT1	MT2	FC1	FC2	GE	DR
Primary up-reserve	15.0	15.0	10.0	10.0	20.0	15.0	15.0	10.0	10.0	20.0	–
Primary down-reserve	11.5	11.5	7.6	7.6	15.3	11.5	11.5	7.6	7.6	15.3	–
Secondary up-reserve	–	–	–	–	86.7	–	–	–	–	–	105.6
Secondary down-reserve	–	–	–	15.8	37.8	11.5	11.5	7.6	7.6	15.3	–
Energy	41.5	41.5	90	90	72.8	41.5	41.5	27.6	27.6	50.3	147.2
Scenario 2											
Primary generation	56.5	56.5	100	100	92.8	56.5	56.5	37.6	37.6	70.3	147.2
Secondary generation	39.6	41.5	90	90	151.5	39.5	30	27.6	27.6	35	252.8
Reference power set-point	39.6	41.5	90	90	151.5	39.5	30	27.6	27.6	35	252.8
$ROCOF_g$	−0.5	−0.5	−0.37	−0.37	−0.6	−0.5	−0.5	−0.37	−0.37	−0.6	–
Scenario 15											
Primary generation	30	30	82.3	82.3	57.5	30	30	20	20	35	147.2
Secondary generation	39.6	41.5	90	76	35	30	30	20	20	35	147.2
Reference power set-point	39.6	41.5	90	76	35	30	30	20	20	35	147.2
$ROCOF_g$	0.38	0.38	0.28	0.28	0.45	0.38	0.38	0.28	0.28	0.45	–

dispatched DG units in providing the microgrid energy requirements, the daily operation cost corresponding to the primary control reserve deployment has been also reduced by 11727.10 cents day^{-1}. Totally, the day-ahead operational costs have been considerably reduced in case 2 which is about 81338.56 cents day^{-1}. The hourly amounts of the provided energy are depicted in Fig. 9. The optimized values of the scheduled primary and secondary control reserves in both cases are represented by Figs. 10 and 11, respectively. The amounts of the downward control reserves are shown by negative values. Clearly, the scheduled downward reserves are in accordance to the positive frequency excursions. In the secondary control level, the MGCC calls the DRPs to supply the scheduled control reserves such that not only the microgrid frequency has been restored at its rated value but also the economic and environmental requirements have been assured.

5. Discussion

For the sake of a detailed analysis, the optimization results at hour 21 are evaluated. According to Tables 3 and 4, the optimization values of the TEF and RCF indices have been increased in case 2 by 86.079 mHz and 1.664 Hz/s, respectively. This is due to that the DR resources have not been participated into the primary frequency control level. Conversely, the consideration of the DR programs in providing the energy and secondary control reserves in case 2 causes the TOC and TOE indices to be decreased within 43772.05 cents and 426.46 kg, respectively. Remarkably, in case 2, the stress of the involuntary load shedding has been lessen about 41.21 kW h. This is due to that in some scenarios specially the low probable ones, the MGCC has scheduled the microgrid required reserves by exploitation the DR resources instead of putting the involuntary load shedding stress on the consumers.

To provide an in-depth optimization assessment, the numerical results at hour 12 are evaluated during two scenarios. The operational characteristics of the two considered scenarios, i.e. scenarios 2 and 15 are given in Table 6. Besides, the optimization results at hour 12 and during the scenarios 2 and 15, corresponding to the provided energy, the scheduled and deployed primary and secondary control reserves as well as the MGCC reference power set-points are illustrated in Table 7.

According to Eq. (20), the values of the primary frequency excursion in both case-studies, in scenarios 2 and 15 can be easily calculated as the following:

$$\Delta f^{2}_{pri,12} = -\frac{93.2 - 23.4 - (-6.99) - 6.76}{9.32 + \frac{1}{0.01} + \frac{1}{0.01} + \frac{1}{0.015} + \frac{1}{0.015} + \frac{1}{0.0075}} = -0.14712\ \text{Hz}$$

$$\Delta f^{15}_{pri,12} = -\frac{-23.3 - 23.4 - 6.99}{7.38 + \frac{1}{0.01} + \frac{1}{0.01} + \frac{1}{0.015} + \frac{1}{0.015} + \frac{1}{0.0075}} = +0.11326\ \text{Hz}$$

Likewise, the amounts of the rate of change of microgrid frequency in scenarios 2 and 15 can be calculated on the basis of the optimization results given in Table 7 and using Eq. (16) as the following:

$$ROCOF^{2}_{MG,12} = -\frac{(60)(15+15+10+10+20)}{2(6)(150)+2(6)(150)+2(8)(100)+2(8)(100)+2(5)(200)} = -0.4772\ \text{Hz/sec}$$

$$ROCOF^{15}_{MG,12} = -\frac{(60)(-11.5-11.5-7.6-7.6-15.3)}{2(6)(150)+2(6)(150)+2(8)(100)+2(8)(100)+2(5)(200)} = +0.3647\ \text{Hz/sec}$$

As it is obvious in Table 7, in scenario 2, the microgrid primary frequency excursion is negative, therefore, the DG units have

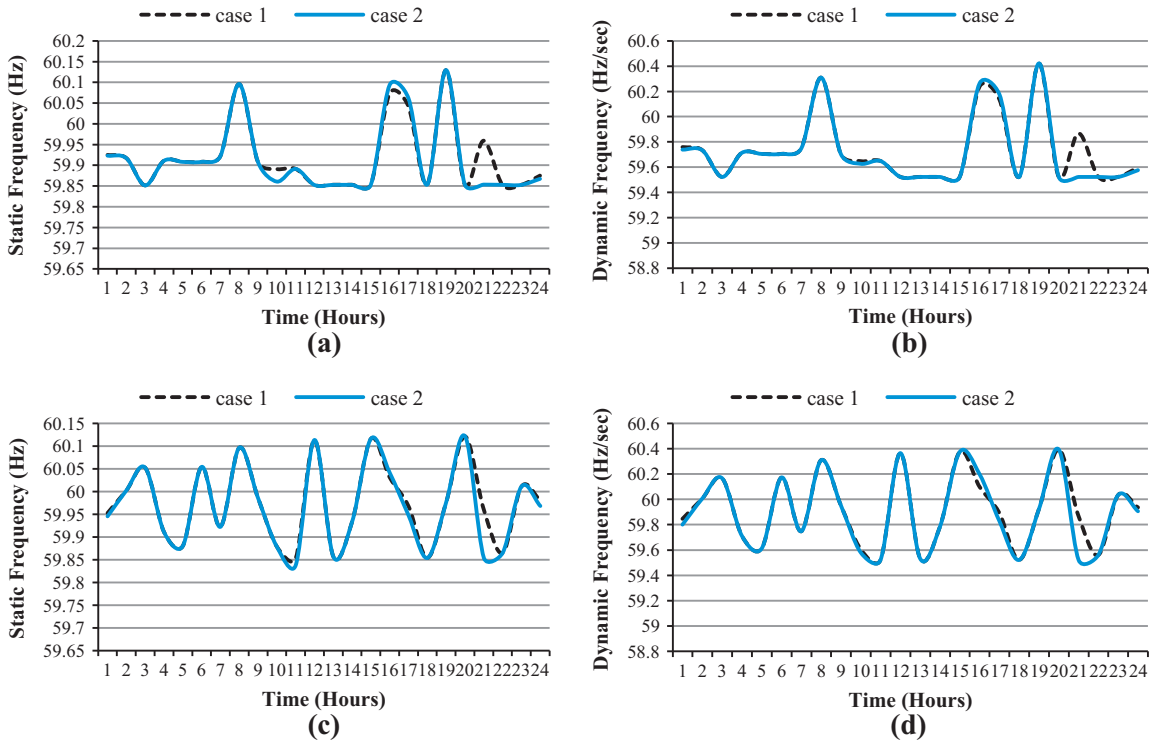

Fig. 12. Microgrid static and dynamic daily RMS-frequency profiles scenario 2 (a and b) and scenario 15 (c and d).

increased their active power generations to alleviate the frequency excursion. In other words, the scheduled up-ward control reserves have been deployed. In contrast in scenario 15 where the microgrid frequency rises within 0.113 mHz, the downward control reserves have been deployed and consequently the DG units have decreased their active power generations. The striking note that should be mentioned is that in case 2, the MGCC has dispatched the energy requirements with lower cost and emission level. In other words, comparing to case 1, by exploitation of the DR resources in case 2, the MGCC has reduced the amount of the dispatched active power associated to the expensive DG units, i.e. the FCs by $2 \times (90–27.6) = 124.8$ kW. Additionally, to reduce the amount of the produced CO_2, the dedicated power generation corresponding to the GE has also been decreased within 22.5 kW. Thus, in case 2 and comparing to case 1, due to the lower dispatched values of the DG units, the cost of the primary control reserves has been reduced within 584.7 cents in both considered scenarios. Observably, the reference power set-points have been adjusted such that the microgrid frequency regulated at 60 Hz. Therefore, in scenario 2 where the frequency drops, the MGCC has to increase the total pre-specified reference power set-points of the DG units within 76.8 kW in case 1. However, interestingly, in case 2, not only the DG unit reference power set-points have not been increased but also the MGCC has decreased the total set-points of the DG units within 28.8 kW. Lieu, the frequency drop has been compensated by appropriately utilization of the DR resources capability in the load reduction within 105.6 kW. Conversely, in scenario 15 due to growth in the microgrid frequency, the MGCC has to decrease the total reference power set-points of the DG units within 53.5 kW in case 1. In case 2, because of the minimum limitations of the active power generation of the DG units, the power consumption reduction associated to the DR resources has been remained unchanged during the secondary control level. Therefore, again the MGCC had to reduce the reference power set-points of the DG units within 53.5 kW. Lastly, it should be noted that the microgrid hourly frequency and ROCOF have been adjusted securely such a way as illustrated by Fig. 12 both the static and dynamic security have been cost-effectively managed in accordance to the required technical margins and their calculated Root Mean Square (RMS) values. The microgrid static and dynamic daily RMS-frequency profiles in the considered scenarios 2 and 15 are shown in Fig. 12. Observably, the derived frequency profiles verify the optimization results given in Tables 3 and 4.

6. Conclusions

One the great challenges of the islanded microgrids is the optimal frequency security management. Procurement of appropriated ancillary services such that the microgrid security is managed in accordance to the economic and environmental purposes is significant control function which should be tracked by means of the MGCC. The paper dealt with a hierarchical energy management system that precisely modeled the microgrid frequency control functions. The static and dynamic performances of the DG units have been formulated based on the droop control and virtual inertia concepts. Besides, it has been considered that the microgrid loads can participate into the proposed frequency management approach using their natural elasticity and in the light of the ancillary service demand response program. To cover the uncertainties stem from the WT/PV and load consumption fluctuations, a MCS-based scenario-based stochastic programming methodology has been employed. The numerical results demonstrate that the demand response programs have a great impact on economizing the micorgrid frequency security provision. The MGCC can reduce the daily operational cost and emission by appropriately management the DR and DG resources. The microgrid operation has been precisely evaluated by the proposed TEF, RCF, TOC and TOE indices. The proposed novel objective function was formulated such that both the static and dynamic frequency profiles of the microgrid were controlled subject to the MGCC cost and emission policies. The optimization results corresponding to the procured energy, primary and secondary control reserves effectively verify the

impressiveness of the proposed security enhancement framework. The MGCC adjusted the reference power set-points associated to the DR and DG resources such that not only the static and dynamic security requirements have been assured but also the microgrid cost and emission targets have been satisfied reasonably. Moreover, by taking the DR programs into account, the stress of involuntary load shedding has been reduced significantly and the DG capacities have been managed with higher degrees of freedom. The implemented frequency dependent energy management system gave an insight perspective to the MGCC for control the microgrid security by properly trading-off between technical and economical issues.

References

[1] Lasseter RH, Paigi P. Microgrid: a conceptual solution. In: Proceeding of 35th annual IEEE power electronics specialists conference; 2004. p. 4285–90.
[2] Katiraei F, Iravani R, Hatziargyriou N, Dimeas A. Microgrids management. IEEE Power Energy Mag 2008;6(3):54–65.
[3] Hatziargyriou N, Asano H, Iravani R, Marnary C. Microgrids. IEEE Power Energy Mag 2007;5(4):78–94.
[4] Olivares DE, Canizares CA, Kazerani M. A centralized energy management system for isolated microgrids. IEEE Trans Smart Grid 2014;5(4):1864–75.
[5] Vandoorn TL, Vasquez JC, Kooning JD, Guerrero JM, Vandevelde L. Microgrids: hierarchical control and on overview of the control and reserve management strategies. IEEE Ind Electron Mag 2013:42–55.
[6] Abdolaziz MMA, El-Saadany EF. Maximum loadability consideration in droop controlled islanded microgrids optimal power flow. Electric Power Syst Res 2014;106:168–79.
[7] Jimeno J, Anduaga J, Oyarzabal J, de Muro AG. Architecture of a microgrid energy management system. Eur Trans Electr Eng 2011;21:1142–58.
[8] Dou C-Xia, Liu B. Multi-agent based hierarchical hybrid control for smart microgrids. IEEE Trans Smart Grids 2013;4(2):771–8.
[9] Lopez JAP, Moreira CL, Madureira AG. Defining control strategies for microgrids islanded operation. IEEE Trans Power Syst 2006;21(2):916–24.
[10] Guerrero JM, Chandorkar M, Lee TL, Loh PC. Advanced control architecture for intelligent microgrids-part I: decentralized and hierarchical control. IEEE Trans Industr Electron 2013;60(4):1254–62.
[11] Guerrero JM, Vasquez JC, Matas J, de Vicuna LG, Castilla M. Hierarchical control of droop-controlled AC and DC microgrids – a general approach toward standardization. IEEE Trans Industr Electron 2011;58(1):387–405.
[12] Justo JJ, Mwasillu F, Lee J, Jung JW. AC-microgrids versus DC-microgrids with distributed energy resources: a review. Renew Sustain Energy Rev 2013;24:387–405.
[13] Rocabert J, Luna A, Blaabjerg F, Rudriguez P. Control of power converters in AC microgrids. IEEE Trans Power Electron 2012;27(11):4734–49.
[14] Bidram A, Davoudi A. Hierarchical structure of microgrids control system. IEEE Trans Smart Grid 2012;3(4):1963–76.
[15] US department of energy. Benefits of demand response in electricity markets and recommendations for achieving them. Report to US congress; 2006. <http://eetd.lbl.gov/EA/EMS/reports/congress-1252d.pdf>.
[16] Faria P, Vale Z. Demand response in electrical energy supply: an optimal real time pricing approach. Energy 2011;36:5374–84.
[17] Moghaddam AA, Seifi A, Niknam T, Alizadeh Pahlavani MR. Multi-objective operation management of a renewable microgrid with back-up micro-turbine/fuel cell/battery hybrid power source. Energy 2011;36:6490–507.
[18] Chen C, Duan S, Cai T, Liu B, Hu G. Smart energy management strategy for optimal microgrid economic operation. IET Renew Power Gener 2011;5(3):258–67.
[19] Mohammad FA, Koivo HN. Online management genetic algorithms of microgrid for residential application. Energy Convers Manage 2012;64:562–8.
[20] Motavasel M, Seifi AR. Expert energy management of a microgrid considering wind energy uncertainty. Energy Convers Manage 2014;83:58–72.
[21] Mohammadi S, Soleymani S, Mozafari B. Scenario-based stochastic operation management of microgrid including wind, photovoltaic, micro-turbine, fuel cell and energy storage devices. Int J Electr Power Energy Syst 2014;54:525–35.
[22] Niknam T, Azizipanah R, Narimani MR. An efficient scenario-based stochastic programming framework for multi-objective optimal microgrid operation. Appl Energy 2012;99:455–70.
[23] Marzband M, Sumper A, Ruiz-Alvarez A, Garcia JLD, Tomoiuga B. Experimental evaluation of a real time energy management system for stand-alone microgrids in day-ahead markets. Appl Energy 2013;106:365–76.
[24] Marzband M, Sumper A, Garcia JLD, Ferret RG. Experimental validation of a real time energy management system for microgrids in islanded mode using a local day-ahead electricity market and MINLP. Energy Convers Manage 2013;76:314–22.
[25] Conti S, Nicolosi R, Rizzo SA, Zeineldin HH. Optimal dispatching of distributed generators and storage systems for MV islanded microgrids. IEEE Trans Power Delivery 2012;27(3):1243–51.
[26] Zakariazadeh A, Jadid S, Siano P. Economic-environmental energy and reserve scheduling of smart distribution systems: a multi-objective mathematical programming approach. Energy Convers Manage 2014;78:151–64.
[27] Zakariazadeh A, Jadid S, Siano P. Stochastic multi-objective operational planning of smart distribution systems considering demand response programs. Electric Power Syst Res 2014;111:156–68.
[28] Rezaei N, Kalantar M. Economic-environmental hierarchical frequency management of a droop controlled islanded microgrid. Energy Convers Manage 2014;88:498–515.
[29] Eid BL, Rahim NA, Selvaraj J, Al Khateb AH. Control methods and objectives for electronically coupled distributed energy resources in microgrids: a review. IEEE Syst J 2014 [early access].
[30] Tsikalakis AG, Hatziargyriou ND. Centralized control for optimizing microgrids operation. IEEE Trans Energy Convers 2008;23(1):241–8.
[31] Galiana FD, Bouffard F, Arroyo JM, Restrepo JF. Scheduling and pricing of coupled energy and primary, secondary and tertiary reserves. Proc IEEE 2005;93(11):1970–83.
[32] machowski J, Bialek JW, Bumby JR. Power system dynamics and stability. Chichester, U.K.: Willey; 1997.
[33] Wood AJ, Wollenberg BF. Power generation, operation and control. New York: Willey; 1984.
[34] Billinton R, Allan RN. Reliability evaluation of power systems. New York, USA: Plenum; 1996.
[35] Wu L, Shahidehpour M, Li T. Cost of reliability analysis based on stochastic unit commitment. IEEE Trans Power Syst 2008;23(3):1364–74.
[36] Ortega-Vazquez MA, Kirschen DS. IEEE Trans Power Syst 2009;24(1):114–24. <http://ieeexplore.ieee.org/search/searchresult.jsp?searchWithin =p_Authors:.QT.Kirschen,%20D.S.QT.&searchWithin=p_Author_Ids:37272580200 &new search=trueEstimating the Spinning Reserve Requirements in Systems With Significant Wind Power Generation Penetration>.
[37] Aghaei J, Karami M, Muttaqi KM, Shayanfar HA, Ahmadi A. MIP-based stochastic security-constrained daily hydrothermal generation scheduling. IEEE Syst J 2014 [early access].
[38] Zhao M, Chen Z, Blaabjerg F. Probabilistic capacity of a grid connected wind farm based on optimization method. Renewable Energy 2006;31:2171–87.
[39] Palensky P, Dietrich D. Demand-side management: demand response, intelligent energy systems and smart loads. IEEE Trans Industr Inf 2011;7(3):381–8.
[40] Garcia AM, Bouffard F, Kirschen DS. Decentralized demand side control contribution to primary frequency control. IEEE Trans Power Syst 2011;26(1):411–9.
[41] Esmaili M, Amjady N, Shayanfar HA. Stochastic congestion management in power markets using efficient scenario approaches. Energy Convers Manage 2010;51:2285–93.
[42] Siano P. Demand response and smart grids – a survey. Renew Sustain Energy Rev 2014;30:461–78.
[43] Albadi MH, El-Saadany EF. A summary of demand response in electricity markets. Electric Power Syst Res 2008;78:1989–96.
[44] Aghaei J, Alizadeh MI. Demand response in smart electricity grids equipped with renewable energy sources: a review. Renew Sustain Energy Rev 2013;18:64–72.
[45] http://www.ferc.gov/industries/electric/indus-act/demand-response/dem-res-adv-metering.asp.
[46] Sioshansi FP. Smart grid: integrating renewable, distributed and efficient energy. Elsevier publications, Part II: Smart supply; 2012. 209–33.
[47] Shi L, Luo Y, Tu GY. Bidding strategy of microgrid with consideration of uncertainty for participating in power market. Int J Electr Power Energy Syst 2014;59:1–13.
[48] Jiang Q, Xue M, Geng G. Energy management of microgrid in grid-connected and islanded modes. IEEE Trans Power Syst 2013;28(3):3380–9.
[49] Generalized Algebraic Modeling Systems (GAMS). <http://www.GAMS.com>.